applied sciences

MDPI

Article

An Extended Proxy-Based Sliding Mode Control of Pneumatic Muscle Actuators

Wei Zhao [1], Aiguo Song [1,*] and Yu Cao [2]

[1] School of Instrument Science and Engineering, Southeast University, Nanjing 210096, China; zhaowei@yijiahe.com

[2] School of Artificial Intelligence and Automation, Huazhong University of Science and Technology, Wuhan 430074, China; cao_yu@hust.edu.cn

* Correspondence: a.g.song@seu.edu.cn; Tel.: +86-25-8379-3293

Received: 24 March 2019; Accepted: 12 April 2019; Published: 16 April 2019

check for updates

Abstract: To solve the problem of controlling an intrinsically compliant actuator, pneumatic muscle actuator (PMA), this paper presents an extended proxy-based sliding mode control (EPSMC) strategy. It is well known that the chattering phenomenon of conventional sliding mode control (SMC) can be effectively solved by introducing a proxy between the physical object and desired position, which results in the so-called proxy-based sliding mode control (PSMC). To facilitate the theoretical analysis of PSMC and obtain a more general form of controller, a new virtual coupling and a SMC are used in our proposed EPSMC. For a class of second-order nonlinear system, the sufficient conditions ensuring the stability and passivity are obtained by using the Lyapunov functional method. Experiments on a real-time PMA control platform validate the effectiveness of the proposed method, and comparison studies also show the superiority of EPSMC over the conventional SMC, PSMC, and PID controllers.

Keywords: pneumatic muscle actuator (PMA); extended proxy-based sliding mode control (EPSMC); stability; passivity; tracking control

1. Introduction

Patients that survive after stroke often suffer from paralysis, and they still want to be productive members of society. Rehabilitation robotics can be considered a specific focus of biomedical engineering and a part of human–robot interaction, increasing the ease of activities in the daily lives of these patients [1,2]. Huang et al. [3] proposed an interval type-2 fuzzy logic control of a mobile two-wheeled inverted pendulum, which is a promising method for future personal mobilities. Wakita et al. [4] and Nakagawa et al. [5] developed a walking intention-based motion control of omnidirectional type cane robot for rehabilitation of the elderly. For most stroke patients undergoing the rehabilitation process, a low-cost home-based rehabilitation solution is of great benefit and therefore in great demand [6–8]. Previous researchers have used robotics in rehabilitation devices because they can automate to perform traditional therapy methods repetitively. However, the drawbacks of robotics, such as space, price, substantial workspace, and especially noncompliance with human hand movements, still limit the applications of the system. As a result, a small, inexpensive hand and forearm rehabilitation device with human compliance is needed for stroke patients. Compared with motors which are commonly used in rehabilitation robots, pneumatic muscle actuators (PMAs) have several merits including intrinsic compliance, low cost, light weight, very high power-to-weight and power-to-volume ratios, etc. [9–11]. So far, a large number of rehabilitation robots driven by PMAs can be found in the literature [12–16].

It should be pointed out that the accurate joint trajectory tracking control of a rehabilitation robot is the basis of a variety of robot-assisted rehabilitation exercises. It can be directly used for passive training on patients with weak active motor ability. This control demand relies heavily on the accurate control of the actuators, including PMAs, discussed in this study. Dao et al. [17] presented an assist-as-needed control of a PMA-based robotic orthosis for gait rehabilitation.

Although PMAs are very good solutions for driving the rehabilitation robots, their control design remains a great challenge. This is because PMAs have characteristics of strong nonlinearity, time-varying parameters, hysteresis, etc. These features jeopardize the control performance of a closed-loop system which is actuated by PMAs. To solve this problem, both model-free and model-based control strategies have been studied for PMAs in recent decades. The PID controller is a typical model-free controller extensively used for PMAs. For stroke rehabilitation, an exoskeleton robotic arm has been built by Xiong et al. [16]. A feedback and feedforward PID controller was used to calculate the desired outputs of the robotic arm. Van Damme et al. established an assistive pneumatic manipulator to help with handling heavy loads [18]. A PID controller is used in this system to correct disturbances and model inaccuracies. Despite the easy implementation, the PID control lacks sound theoretical foundations for convergence analysis. In addition, the coefficients adjustment of the PID controller is also time-consuming. Another kind of model-free controller is realized by soft-computing techniques, e.g., fuzzy sets, artificial neural networks (ANNs), etc. Zhang et al. proposed a hybrid fuzzy controller composed of a bang-bang controller and fuzzy controller for a novel curved pneumatic muscle-based rotary actuator for the wearable elbow exoskeleton [19]. Xie et al. [20] proposed an iterative fuzzy controller for PMA-driven rehabilitation robot. Chang [21] showed an adaptive self-organizing fuzzy sliding mode controller (SMC) for a 2-DOF PMA-driven rehabilitation robot. Jamwal et al. presented the development of a novel adaptive wearable ankle robot for the treatments of ankle sprain through physical rehabilitation [22]. In their study, an adaptive fuzzy logic controller based on Mamdani inference has been developed and appended with the fuzzy-based disturbance observer (FBDO) to compensate for the transient nature of the PMA. Huang et al. proposed several model predictive control (MPC) methods for PMAs based on ANNs [23,24]. In their work, the uncertain PMA model was approximated by the echo state networks (ESNs) so that the MPC control strategy obtained very high accurate control performance. Although the soft-computing techniques are proved to be capable of approximating arbitrary nonlinear characteristics, the requirement of large storage space and high computation ability confines the real-time and compact PMA control applications.

In the case of the model-based controller, Wu et al. applied the dynamic surface control (DSC) characterized by convenient design and good transient performance for realizing pneumatic muscle (PM) tracking control [25]. In [26], a Maxwell-slip model used as a lumped-parametric quasi-static model is proposed to capture the force/length hysteresis of a PMA. The obtained model is simple but physically meaningful and easy to handle in terms of control. The main challenge of model-based controllers for PMAs is that the identified model parameters are highly uncertain. This demands strong robustness of the controllers for PMAs. The SMC might be a suitable solution due to its high robustness to both internal system uncertainties and external disturbances. Shen developed a fully nonlinear model that encompasses all the major nonlinearities in a PMA-actuated servo system [27]. Based on this model, a SMC is developed to obtain robust control in the existence of model uncertainties and disturbances. Xing et al. used the sliding mode approach to the tracking control problem of a planar arm manipulator system driven by a new type of actuator, which comprises a PMA and a torsion spring [28]. Cao et al. [29] applied a SMC for PMA-based gait rehabilitation exoskeleton for verifying the compliance of the exoskeleton. Aschemann and Schindele presented a cascaded SMC scheme for a new pneumatic linear axis which could be seen as an alternative to an electric direct linear drive [30]. On the other hand, it should be noted that the SMC has a "chattering" problem which may bring damages to practical actuators.

Recently, a proxy-based sliding mode control (PSMC) approach has been proposed as a safe extension of PID control and is the simplest type of SMC. The PSMC can produce overdamped resuming motion from large positional errors without sacrificing tracking accuracy during normal operation. Also, the "chattering" phenomenon in conventional SMC is avoided by introducing the so-called "proxy". Due to these advantages, the PSMC is widely applied not only in PMA applications [31] but also many other control fields [32]. However, the stability analysis of original PSMC is based on a strict conjecture of local passivity of well-tuned PID controller [32]. There is much room to improve in the view of the point of the general theoretical framework. Also, the basic idea of designing PID-type virtual coupling between the proxy and physical object can be generally extended in our opinion.

In this study, we propose a novel PSMC with elaborately designed couple force between the proxy and object. Based on this technique, the Lyapunov stability of proposed PSMC can be analyzed straightforwardly by using the passivity approach. Furthermore, we successfully applied the approach in a real PMA control platform. By using this new PSMC, better performance can be achieved compared with some conventional control approaches. Since the proposed method presents well in the PMA tracking control, it has a good prospect of becoming an excellent pneumatic rehabilitation robot control approach. This will result in a safe and quantitative passive training implemented by the rehabilitation robot.

The rest of paper is organized as follows. Section 2 gives the dynamic model of PMA. The controller design and stability analysis are presented in Section 3. In Section 4, the experimental studies are given, in which we compare the proposed controller and conventional SMC and PSMC. This study is finally concluded in Section 5.

2. Dynamics of PMA

So far, except the FESTO AG Company's demonstrations, PMAs have not been standardized as commercial products and in applications containing such actuators. Therefore, it is of great importance to choose suitable PMA that fits the application and use the correct mathematical PMA model. The high nonlinearities due to the existence of the pressurized air, the elastic-viscous material and the geometric features of PMA are the first problem that a control engineer has to deal with in order to derive and use a proper PMA mathematical model.

Two main categories for the mathematical models of a PMA are prevalent: the theoretical and the phenomenological models. The theoretical models, which are derived from the law of energy conservation, describe the PMA behavior based on quasi-static states without the inclusion of explicitly temporal information. However, this approach limits its application for real-time control. This is because it is too complex in structure and requires too many parameters that are difficult to obtain during experimentation.

In this study, we adopt a phenomenological model as a combination of effects from nonlinear friction, spring and contraction components to describe the dynamic behavior of a PM pulling a mass against gravity (shown in Figure 1).

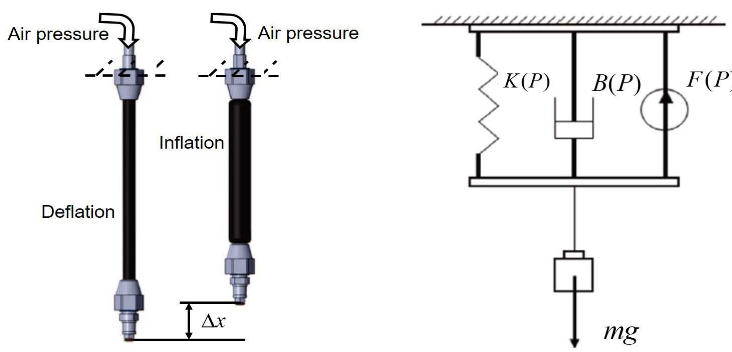

Figure 1. The FESTO PMA and their three-element models.

The coefficients related to these three elements depend on the input pressure of the PM. The equations describing approximately the dynamics of a PM are given by:

$$M\ddot{x} + B(P)\dot{x} + K(P)x = F(P) - Mg \tag{1}$$

$$K(P) = K_0 + K_1 P \tag{2}$$

$$B(P) = B_{0i} + B_{1i}P(\text{inflation}) \tag{3}$$

$$B(P) = B_{0d} + B_{1d}P(\text{deflation}) \tag{4}$$

$$F(P) = F_0 + F_1 P \tag{5}$$

where M is the mass of PMA. g denotes the acceleration of gravity. P is used to denote the input pressure. $x = 0$ corresponds to the fully deflated position of PMA, and the coefficients $K(P)$ and $B(P)$ are pressure-dependent representing the spring and the damping elements, respectively. The contractile element presented the effective force $F(P)$. The damping coefficient depends on whether the PM is inflated and deflated.

From Equation (1), the dynamics of PMA can be rewritten as the following standard single-input-single-output (SISO) second-order nonlinear system:

$$\ddot{x} = f(x, \dot{x}) + b(x, \dot{x})u(t) + d(x, \dot{x}, t) \tag{6}$$

where

$$f(x, \dot{x}) = \frac{1}{M}\left[F_0 - B_0\dot{x} - K_0 x - Mg\right], \tag{7}$$

$$b(x, \dot{x}) = \frac{1}{M}\left[F_1 - B_1\dot{x} - K_1 x\right], \tag{8}$$

and

$$\begin{cases} B_0 = B_{0i}, B_1 = B_{1i} & if \;\; \dot{x} > 0 \;\; (\text{inflation}) \\ B_0 = B_{0d}, B_1 = B_{1d} & if \;\; \dot{x} < 0 \;\; (\text{deflation}) \\ B_0, B_1 \;\; \text{hold} & if \;\; \dot{x} = 0 \end{cases} \tag{9}$$

In Equation (6), it should be noticed that all the uncertainties including modeling errors and external disturbances are lumped into a single term $d(x, \dot{x}, t)$.

3. Controller Design and Stability Analysis

In the conventional PSMC strategy, an imaginary object called "proxy" is introduced to reduce the "chattering" phenomenon caused by the sign function in classical SMC. A proxy is a virtual object which is connected to both the desired position and the physical actuator, and the connection between the actuator and proxy is the so-called "virtual coupling". Since the virtual coupling is usually designed as a normal PID-type controller, the sign function does not directly affect the physical object so that the "chattering" can be reduced to a great extent. In addition, the PID-type coupling controller can also guarantee that the error between the proxy and physical object will be finally convergent to zero. On the other hand, the standard SMC is adopted between the proxy and the desired position. That is, the SMC is directly exerted on the proxy, which results in the stability and robustness of the whole system.

Although the PSMC has been successfully applied in many applications, there is still much room to improve especially in the theoretical stability analysis. This is because the conventional PSMC is intrinsically a model-free controller so that its stability condition is based on a strong conjecture (see [32]).

3.1. Extended Proxy-Based SMC Design

In this study, we extended the idea of conventional PSMC to a general nonlinear system which is described by the SISO second-order model (6). The main idea of our controller design is to add the model-based compensation to the PID-type virtual coupling controller and propose a new SMC strategy for controlling the proxy. The comparison between the conventional PSMC and our EPSMC is shown in Figure 2.

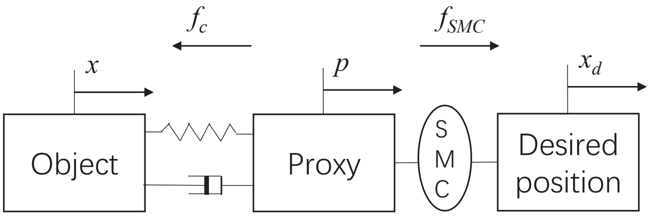

Figure 2. The physical interpretation of proposed EPSMC.

In Figure 2, the masses of object (PMA) and proxy are M and m_p, respectively. x, p, x_d are used to denote the positions of object, proxy, and reference. f_c means the virtual coupling force between the proxy and physical object, and f_{SMC} is the sliding mode controller for controlling the proxy to approach the reference trajectory. To obtain a stable extended PSMC for the nonlinear system (6), we design the following novel sliding manifolds:

$$\begin{cases} \sigma_p = \dot{x}_d - \dot{p} + H(x_d - p) + I\int(x_d - p)\,dt \\ \sigma_x = \dot{x}_d - \dot{x} + H(x_d - x) + I\int(x_d - x)\,dt \end{cases} \tag{10}$$

Unlike the conventional PSMC, the proposed sliding mode manifolds contain integrals of $x_d - p$ and $x_d - x$, which play important roles in reducing the steady error in the tracking control. Furthermore, we also design new virtual coupling force f_c and sliding mode controller f_{SMC} as:

$$\begin{cases} f_c = \frac{1}{b}\left[K_P(p - x) - f + \ddot{x}_d + H(\dot{x}_d - \dot{x}) + I(x_d - x)\right] \\ f_{SMC} = \Gamma \mathrm{sgn}(\sigma_p) - K_P(p - x) + m_p\ddot{x}_d + m_p H(\dot{x}_d - \dot{p}) + m_p I(x_d - p) + \\ \qquad \frac{1}{b}\left[K_P(p - x) - f + \ddot{x}_d + H(\dot{x}_d - \dot{x}) + I(x_d - x)\right] \end{cases} \tag{11}$$

Please note that the proposed virtual coupling force f_c is not a pure PID-type controller. Some terms based on known dynamics are added for the convenience of theoretical analysis. Similar consideration is taken in the design of sliding mode controller f_{SMC}.

3.2. Stability Analysis

By substituting the controllers (11) into the model (6), the closed-loop system model is given by:

$$\begin{cases} \ddot{x} = K_P(p - x) + \ddot{x}_d + H(\dot{x}_d - \dot{x}) + I(x_d - x) + d(t) \\ m_p\ddot{p} = f_{SMC} - f_c = \Gamma \mathrm{sgn}(\sigma_p) - K_P(p - x) + m_p\ddot{x}_d + m_p H(\dot{x}_d - \dot{p}) + m_p I(x_d - p) \end{cases} \tag{12}$$

The stability of the closed-loop system can be analyzed as follows. First, we prove the stability when the lumped disturbance $d = 0$.

Theorem 1. *Consider the system described by (6) with $d = 0$, and the controllers are assumed as (11). The trajectory of system (6) can then be driven onto the sliding mode manifolds (10).*

Proof. Introduce the following quadratic function:

$$V_1 = \frac{1}{2}m_p{\sigma_p}^2. \tag{13}$$

By differentiating the above equation, we have

$$\begin{aligned}
&\dot{V}_1 = \sigma_p m_p \dot{\sigma}_p \\
&= \sigma_p \left(m_p \ddot{x}_d - m_p \ddot{p} + m_p H \left(\dot{x}_d - \dot{p}\right) + m_p I \left(x_d - p\right)\right) \\
&= \sigma_p \left(m_p \ddot{x}_d - \left(\Gamma \mathrm{sgn}\left(\sigma_p\right) - K_P \left(p - x\right) + m_p \ddot{x}_d + m_p H \left(\dot{x}_d - \dot{p}\right) + m_p I \left(x_d - p\right)\right)\right. \\
&\left. + \, m_p H \left(\dot{x}_d - \dot{p}\right) + m_p I \left(x_d - p\right)\right) \\
&= \sigma_p \left(-\Gamma \mathrm{sgn}\left(\sigma_p\right) + K_P \left(p - x\right)\right) \\
&= -\Gamma \left|\sigma_p\right| + K_P \left(p - x\right)\left(\dot{x}_d - \dot{p}\right) + K_P H \left(p - x\right)\left(x_d - p\right) + K_P I \left(p - x\right) \int \left(x_d - p\right) dt
\end{aligned} \tag{14}$$

Next, introduce another quadratic function:

$$V_2 = \frac{1}{2} {\sigma_x}^2. \tag{15}$$

By differentiating the above equation, it follows from (12) that

$$\begin{aligned}
&\dot{V}_2 = \sigma_x \dot{\sigma}_x \\
&= \sigma_x \left(\ddot{x}_d - \ddot{x} + H \left(\dot{x}_d - \dot{x}\right) + I \left(x_d - x\right)\right) \\
&= \sigma_x \left(\ddot{x}_d - \left(K_P \left(p - x\right) + \ddot{x}_d + H \left(\dot{x}_d - \dot{x}\right) + I \left(x_d - x\right)\right) + H \left(\dot{x}_d - \dot{x}\right) + I \left(x_d - x\right)\right) \\
&= \sigma_x \left(-K_P \left(p - x\right)\right) \\
&= K_P \left(x - p\right)\left(\dot{x}_d - \dot{x}\right) + K_P H \left(x - p\right)\left(x_d - x\right) + K_P I \left(x - p\right) \int \left(x_d - x\right) dt
\end{aligned} \tag{16}$$

Introducing the third quadratic function:

$$V_3 = \frac{1}{2} K_P (p - x)^2 + \frac{1}{2} K_P I \left(\int (p - x)\, dt\right)^2. \tag{17}$$

Similar to V_1 and V_2, we have

$$\dot{V}_3 = K_P \left(p - x\right)\left(\dot{p} - \dot{x}\right) + K_P I \left(p - x\right) \int \left(p - x\right) dt \tag{18}$$

Choose the following Lyapunov function candidate:

$$V = V_1 + V_2 + V_3. \tag{19}$$

The derivative of V can then be calculated by combing (14), (16) and (18). It follows that:

$$\begin{aligned}
&\dot{V} = \dot{V}_1 + \dot{V}_2 + \dot{V}_3 \\
&= -\Gamma \left|\sigma_p\right| - K_P H (p - x)^2 \leq 0
\end{aligned} \tag{20}$$

This completes the proof. □

If there is no disturbance $d(t)$, from Theorem 1 we know that the system trajectory will finally be driven onto the sliding mode manifolds $\sigma_p = 0$ and $\sigma_x = 0$, on which the tracking error $x_d - x$ will converge to zero.

On the other hand, when the lumped disturbance d is unavoidable, the system is found to be passive through the following theorem.

Theorem 2. *The second-order nonlinear system*

$$\begin{aligned}
&\ddot{x} = f(x, \dot{x}) + b(x, \dot{x}) u(t) + d(t) \\
&y = -\sigma_x
\end{aligned} \tag{21}$$

mapping $d(t)$ to y is passive.

Proof. Let us choose the storage function as (19). It can be found that the derivatives of V_1 and V_3 are the same even $d \neq 0$. For V_2, we have

$$\begin{aligned}
&\dot{V}_2 = \sigma_x \dot{\sigma}_x \\
&= \sigma_x \left(\ddot{x}_d - \ddot{x} + H\left(\dot{x}_d - \dot{x}\right) + I\left(x_d - x\right)\right) \\
&= \sigma_x \left(\ddot{x}_d - \left(K_P\left(p - x\right) + \ddot{x}_d + H\left(\dot{x}_d - \dot{x}\right) + I\left(x_d - x\right) + d\right) + H\left(\dot{x}_d - \dot{x}\right) + I\left(x_d - x\right)\right) \\
&= \sigma_x \left(-K_P\left(p - x\right) - d\right) \\
&= K_P\left(x - p\right)\left(\dot{x}_d - \dot{x}\right) + K_P H\left(x - p\right)\left(x_d - x\right) + K_P I\left(x - p\right) \int \left(x_d - x\right) dt - d\sigma_x
\end{aligned} \tag{22}$$

It follows that we have:

$$\begin{aligned}
&\dot{V} = \dot{V}_1 + \dot{V}_2 + \dot{V}_3 \\
&= -\Gamma\left|\sigma_p\right| - K_P H(p - x)^2 + d\sigma_x \leq yd
\end{aligned} \tag{23}$$

Therefore, the necessary condition of system passivity is satisfied. This completes the proof. □

4. Experiment Studies

4.1. Experimental Setup

The experimental setup is explained in this section. All the equipment and hardware is shown in Figure 3. The core part of the PMA control experiment platform is an xPC target, which is a real-time environment solution developed by Mathworks Inc. and is available in MATLAB/Simulink. There are two computers are used in the experiments, including a host computer and a target one. The MATLAB/SIMULINK and C language compiler are installed in the host computer, in which the executable codes are generated and fed into the target computer to run in real time. Table 1 lists the hardware including the sensors, valves, air compressor, and PM used in the experiments.

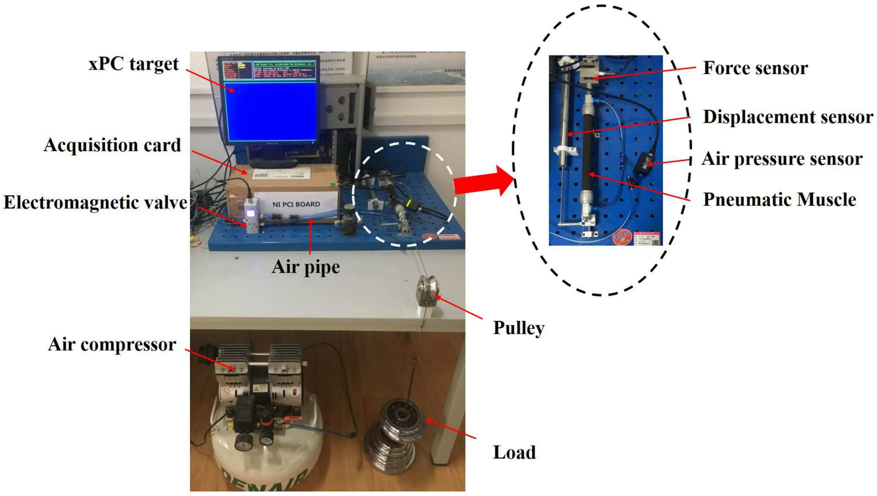

Figure 3. The PMA experimental platform.

To verify the effectiveness of the proposed method, several experiments are designed and performed. The reference trajectory is a sinusoidal signal:

$$x_d = A\sin(2\pi f t) + B \tag{24}$$

where $A = 0.01$ m, $f = 0.3$ Hz, and $B = 0.01$ m. We aim to measure and compare the accuracy of control results. The maximum absolute error and the integral of absolute error can describe the tracking performance from two different perspectives:

$$\begin{aligned} MaxERROR^1 &= Max(|x_d(t) - x(t)|_{t=1}^{n}) \\ InteERROR^2 &= \frac{1}{n}\sum_{t=1}^{n}|x_d(t) - x(t)| \end{aligned} \tag{25}$$

where n is the total sample of the experiment.

Table 1. List of main equipment in the experiments.

Name	Type	Details
Displacement sensor	GA-75	Measurementrange: 0–150 mm Linearity: <0:1% (=0.09%)
Electromagnetic valve	ITV1030-211BS	Input: 0–5 V Output: 0.005–0.5 MPa
Relieve-pressure valve	AW20-02BCG	Regulating range: 0.05–0.85 MPa
Pneumatic Muscle	FESTO DMSP-20-200N-RM	Inner diameter: 20 mm Rated length: 60–9000 mm Lifting force: 0–1500 N
Data acquisition board	NIPCI-6025E	16 AI and 2 AO 32 digital I/O buses Sampling rate: 200 kS/s
Force sensor	TJL-1	Measurement range: 0–300 N Sensitivity: 2 ± 0.1 mV/V Accuracy: 0.03% F· S
Power supply	Q-120DE	Input: AC 200 V, 50 Hz Output: $\pm$5 V, $\pm$12 V, $\pm$24 V
Air compressor	Denair, DW35	Capacity: 150 L Power: 800 W Exhaust pressure: 0.8 MPa

4.2. Experimental Results

To investigate the performance of the proposed method, several experiments have been designed with the reference. First, we compare the control effects of the EPSMC, SMC, PSMC, PID control, and fuzzy control to show the superiority of the proposed method. Then, the ESPMC is applied to the PMA with different loads, by which the robustness of the system would be illustrated.

Figure 4 shows the tracking performance of the PMA. Figure 5 is the result of the corresponding tracking error. The results of the tracking performance are shown in Table 2 which indicates that the EPSMC behaves best since it can reduce the "chattering" phenomenon significantly. Meanwhile, the SMC suffers from the sever "chattering", which results in the inaccurate track. The PSMC and PID are model-free control strategies. As long as the suitable control parameters are adjusted, favorable control performance can be achieved, but this is also its deficiency. In physical applications, it takes a lot of time and effort to select the appropriate parameters. Also, the fuzzy controller is heavily dependent on the experience of selecting membership functions and rules and suffers from high computational burden.

Table 2. The tracking performance of different control strategies.

Strategy	MaxERROR (m)	InteERROR (m)
EPSMC	1.1×10^{-3}	3.3×10^{-4}
SMC	7.9×10^{-3}	2.3×10^{-3}
PSMC	5.9×10^{-3}	1.7×10^{-3}
PID	2.7×10^{-3}	1.1×10^{-3}
Fuzzy Control	4.3×10^{-3}	1.9×10^{-3}

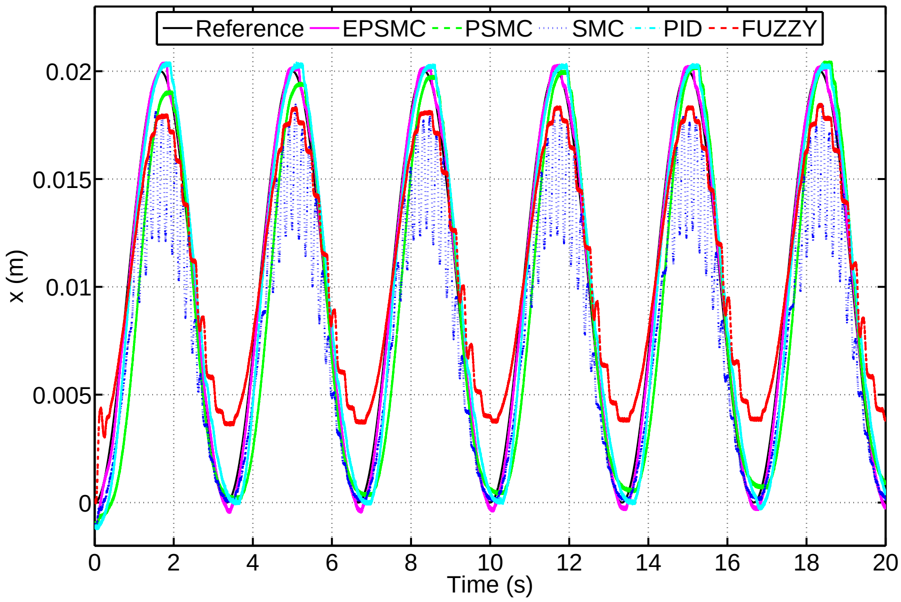

Figure 4. The tracking performance of the PMA.

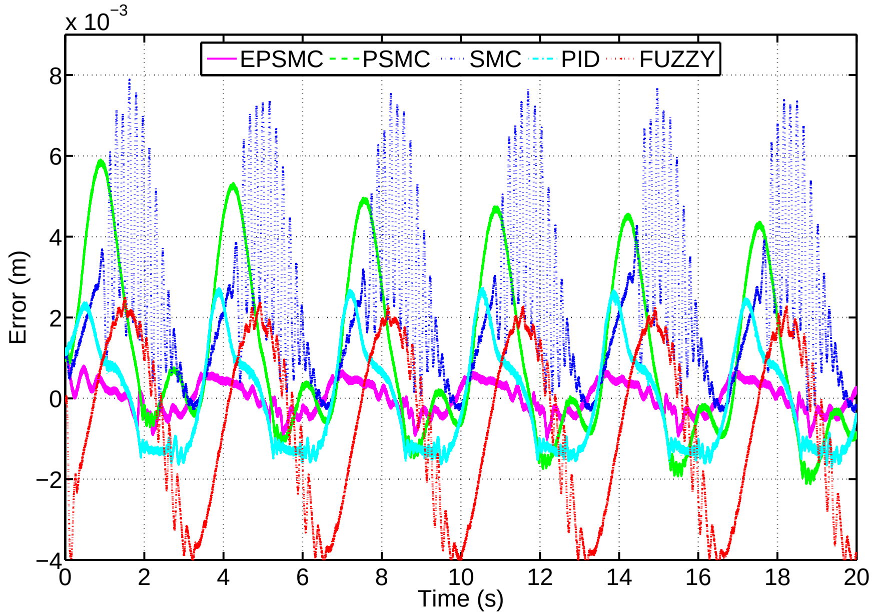

Figure 5. The tracking error of the PMA.

To further investigate the robustness of the proposed method, the PMA is attached to 0.5 kg, 1.0 kg, and 1.5 kg loads and driven to tracking the same reference. Figures 6 and 7 are the performances of PMA tracking. It is shown that even though the PMA is attached to different loads, the control effect is almost the same. Obviously, as the quality increases, the control effect also deteriorates. This is reasonable because the control parameters are tuned based on the PMA that does not mount any mass. The result is shown in Table 3.

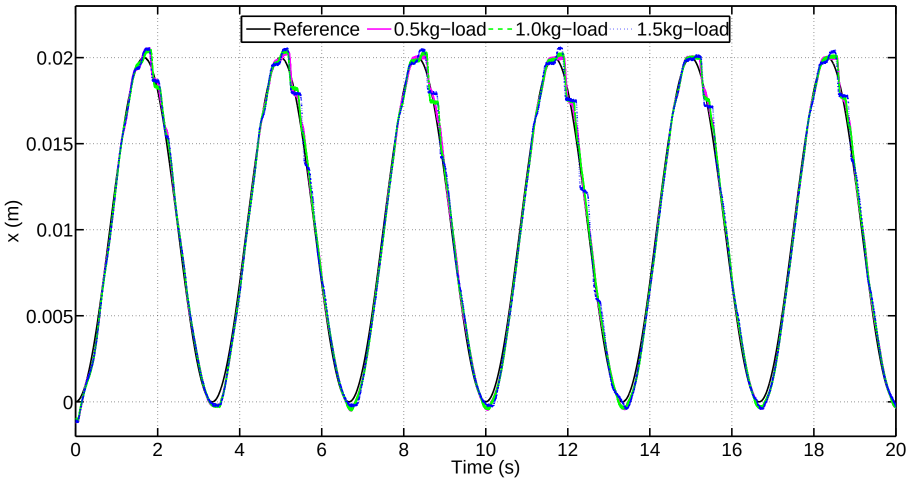

Figure 6. The tracking performance of the PMA with different loads.

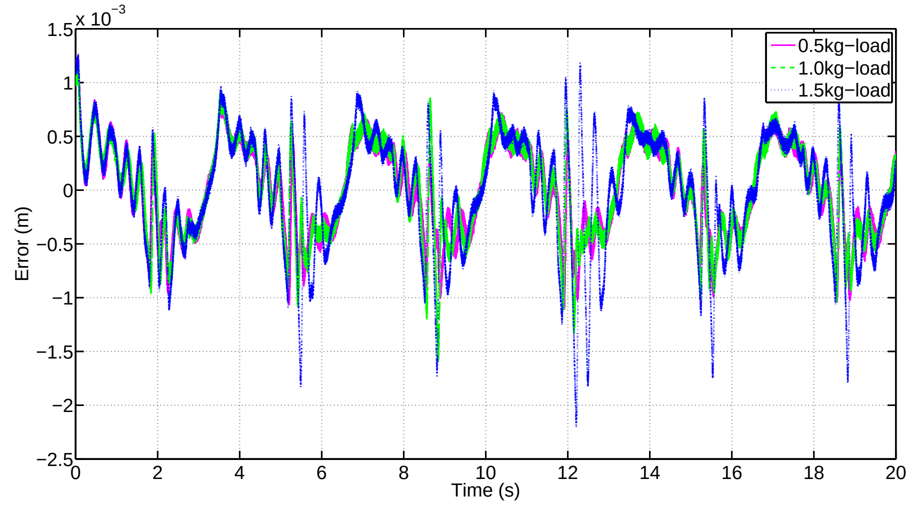

Figure 7. The tracking error of the PMA with different loads.

Table 3. The tracking performance of the EPSMC with different loads.

Weight	MaxERROR (m)	InteERROR (m)
0.5 kg-load	1.2×10^{-3}	3.6×10^{-4}
1.0 kg-load	1.6×10^{-3}	3.8×10^{-4}
1.5 kg-load	2.2×10^{-3}	4.2×10^{-4}

5. Conclusions

As far as the human-friendly robot should be safe for people, especially patients, compliance is a necessary property for such kind of robot. The PMA is promising because it is an essentially soft actuator. Unlike motors, the PMA is driven by compressed air and capable of providing necessary compliance for rehabilitation robots. As a result, it is very suitable for wearable rehabilitation robots, such as exoskeletons. However, due to its nonlinearities, time-varying parameters, and hysteresis, it is difficult to control accurately. The traditional control strategy, such as SMC, suffers from the "chattering" problem. Hence, a new EPSMC strategy is proposed and validated in a real physical PMA experiment platform. The stability and passivity of the EPSMC system are proven based on the Lyapunov theorem, and the strong conjecture which is assumed in the traditional PSMC is then avoided. Comparison of experimental studies in the PMA platform are also conducted. The results show that the proposed method has less "chattering" and better performance compared with the traditional SMC and PSMC methods. Furthermore, the robustness of the proposed method is also verified by experiments using different loads.

Author Contributions: Conceptualization, W.Z. and A.G.S.; methodology, W.Z.; validation, W.Z.; software, Y.C.

Funding: This research was funded by the key research and development project of Jiangsu province grant number BE2018004-4.

Acknowledgments: The authors would like to thank the anonymous reviewers who greatly help to improve this paper.

Conflicts of Interest: The authors declare no conflict of interest.

Abbreviations

The following abbreviations are used in this manuscript:

PMA	Pneumatic Muscle Actuator
SMC	Sliding Mode Control
PSMC	Proxy-based Sliding Mode Control
EPSMC	Extended Proxy-based Sliding Mode Control
PID	Proportional-Integral-Derivative
ANN	Artificial Neural Network
FBDO	Fuzzy-Based Disturbance Observer
MPC	Model Predictive Control
ESN	Echo State Networks
DSC	Dynamic Surface Control

References

1. Hopman, W.M.; Verner, J. Quality of life during and after inpatient stroke rehabilitation. *Stroke* **2003**, *34*, 801. [CrossRef]
2. Huang, J.; Tu, X.; He, J. Design and evaluation of the RUPERT wearable upper extremity exoskeleton robot for clinical and in-home therapies. *IEEE Trans. Syst. Man Cybern. Syst.* **2016**, *46*, 926–935. [CrossRef]
3. Huang, J.; Ri, M.H.; Wu, D.; Ri, S. Interval Type-2 Fuzzy Logic Modeling and Control of a Mobile Two-Wheeled Inverted Pendulum. *IEEE Trans. Fuzzy Syst.* **2018**, *26*, 2030–2038 [CrossRef]
4. Wakita, K.; Huang, J.; Di, P.; Sekiyama, K.; Fukuda, T. Human Walking Intention Based Motion Control of Omni-directional Type Cane Robot. *IEEE/ASME Trans. Mechatron.* **2013**, *18*, 285–296. [CrossRef]
5. Nakagawa, S.; Hasegawa, Y.; Fukuda, T.; Kondo, I.; Tanimoto, M.; Di, P.; Huang, J.; Huang, Q. Tandem Stance Avoidance Using Adaptive and Asymmetric Admittance Control for Fall Prevention. *IEEE Trans. Neural Syst. Rehabil. Eng.* **2016**, 542–550. [CrossRef]
6. Song, A.; Wu, C.; Ni, D.; Li, H.; Qin, H. One-therapist to three-patient telerehabilitation robot system for the upper limb after stroke. *IEEE Trans. Syst. Man Cybern. Syst.* **2016**, *8*, 319–329. [CrossRef]
7. Trujillo, P.; Mastropietro, A.; Scano, A.; Chiavenna, A.; Mrakic-Sposta, S.; Caimmi, M.; Molteni, F.; Rizzo, G. Quantitative EEG for Predicting Upper Limb Motor Recovery in Chronic Stroke Robot-Assisted Rehabilitation. *IEEE Trans. Neural Syst. Rehabil. Eng.* **2017**, *25*, 1058–1067. [CrossRef]
8. Marini, F.; Hughes, C.M.L.; Squeri, V.; Doglio, L.; Moretti, P.; Morasso, P.; Masia, L. Robotic wrist training after stroke: Adaptive modulation of assistance in pediatric rehabilitation. *Robot. Auton. Syst.* **2017**, *91*, 169–178. [CrossRef]
9. Tondu, B.; Lopez, P. Modeling and control of McKibben artificial muscle robot actuators. *IEEE Control Systems* **2000**, *20*, 15–38.
10. Morales, R.; Badesa, F.J.; Garcia-Aracil, N.; Sabater, J.M.; Pérez-Vidal, C. Pneumatic robotic systems for upper limb rehabilitation. *Med. Biol. Eng. Comput.* **2011**, *49*, 1145. [CrossRef]

11. Polygerinos, P.; Lyne, S.; Wang, Z.; Nicolini, L.F.; Mosadegh, B.; Whitesides, G.M.; Walsh, C.J. Towards a soft pneumatic glove for hand rehabilitation. In Proceedings of the 2013 IEEE/RSJ International Conference on Intelligent Robots and Systems, Tokyo, Japan, 3–7 November 2013; pp. 1512–1517.
12. Ohta, P.; Valle, L.; King, J.; Low, K.; Yi, J.; Atkeson, C.G.; Park, Y.-L. Design of a lightweight soft robotic arm using pneumatic artificial muscles and inflatable sleeves. *Soft Robot.* **2018**, *5*, 204–215. [CrossRef] [PubMed]
13. Kang, R.; Guo, Y.; Chen, L.; Branson III, D.T.; Dai, J.S. Design of a pneumatic muscle based continuum robot with embedded tendons. *IEEE/ASME Trans. Mechatron.* **2017**, *22*, 751–761. [CrossRef]
14. Jamwal, P.K.; Hussain, S.; Ghayesh, M.H.; Rogozina, S.V. Impedance control of an intrinsically compliant parallel ankle rehabilitation robot. *IEEE Trans. Ind. Electron.* **2016**, *63*, 3638–3647. [CrossRef]
15. Cui, Y.; Matsubara, T.; Sugimoto, K. Pneumatic artificial muscle-driven robot control using local update reinforcement learning. *Adv. Robot.* **2017**, *31*, 397–412. [CrossRef]
16. Xiong, C.; Jiang, X.; Sun, R.; Huang,X.L.; Xiong, Y.L. Control methods for exoskeleton rehabilitation robot driven with pneumatic muscles. *Ind. Robot Int. J.* **2009**, *36*, 210–220. [CrossRef]
17. Dao, Q.; Yamamoto, S. Assist-as-Needed Control of a Robotic Orthosis Actuated by Pneumatic Artificial Muscle for Gait Rehabilitation. *Appl. Sci.* **2018**, *8*, 499. [CrossRef]
18. Van Damme, M.; Daerden, F.; Lefeber, D. A pneumatic manipulator used in direct contact with an operator. In Proceedings of the 2005 IEEE International Conference on Robotics and Automation, Barcelona, Spain, 18–22 April 2005; pp. 4494–4499.
19. Zhang, J.F.; Yang, C.J.; Chen, Y.; Zhang,Y.; Dong, Y.M. Modeling and control of a curved pneumatic muscle actuator for wearable elbow exoskeleton. *Mechatronics* **2008**, *18*, 448–457. [CrossRef]
20. Xie, S.Q.; Jamwal, P.K. An iterative fuzzy controller for pneumatic muscle driven rehabilitation robot. *Expert Syst. Appl.* **2011**, *38*, 8128–8137. [CrossRef]
21. Chang, M.K. An adaptive self-organizing fuzzy sliding mode controller for a 2-DOF rehabilitation robot actuated by pneumatic muscle actuators. *Control Eng. Pract.* **2010**, *18*, 13–22. [CrossRef]
22. Jamwal, P.K.; Xie, S.Q.; Hussain, S.; Parsons, J.G. An adaptive wearable parallel robot for the treatment of ankle injuries. *IEEE/ASME Trans. Mechatron.* **2014**, *19*, 64–75. [CrossRef]
23. Huang, J.; Qian, J.; Liu, L.; Wang, Y.; Xiong, C.; Ri, S. Echo state network based predictive control with particle swarm optimization for pneumatic muscle actuator. *J. Frankl. Inst.* **2016**, *353*, 2761–2782. [CrossRef]
24. Huang, J.; Cao, Y.; Xiong, C.; Zhang, H.-T. An Echo State Gaussian Process Based Nonlinear Model Predictive Control for Pneumatic Muscle Actuators. *IEEE Trans. on Autom. Sci. Eng.* **2018**. [CrossRef]
25. Wu, J.; Huang, J.; Wang, Y.; Xing, K. Nonlinear Disturbance Observer-Based Dynamic Surface Control for Trajectory Tracking of Pneumatic Muscle System. *IEEE Trans. Control Syst. Eng.* **2014**, *22*, 440–455. [CrossRef]
26. Vo-Minh, T.; Tjahjowidodo, T.; Ramon, H.; Brussel, H.V. A new approach to modeling hysteresis in a pneumatic artificial muscle using the Maxwell-slip model. *IEEE/ASME Trans. Mechatron.* **2011**, *16*, 177–186. [CrossRef]
27. Shen, X. Nonlinear model-based control of pneumatic artificial muscle servo systems. *Control Eng. Pract.* **2010**, *18*, 311–317. [CrossRef]
28. Xing, K.; Huang, J.; He, J.; Wang, Y.; Wu, J.; Xu, Q. Sliding mode tracking for actuators comprising pneumatic muscle and torsion spring. *Trans. Inst. Meas. Control* **2012**, *34*, 255–277. [CrossRef]
29. Cao, J.; Xie, S.Q.; Das, R. MIMO Sliding Mode Controller for Gait Exoskeleton Driven by Pneumatic Muscles. *IEEE Trans. Control Syst. Technol.* **2018**, *26*, 274–281. [CrossRef]
30. Aschemann, H.; Schindele, D. Sliding-Mode Control of a High-Speed Linear Axis Driven by Pneumatic Muscle Actuators. *IEEE Trans. Ind. Electron.* **2008**, *55*, 3855–3864. [CrossRef]
31. Damme, M.V.; Vanderborght, B.; Verrelst, B.; Ham, R.V.; Daerden, F.; Lefeber, D. Proxy-based Sliding Mode Control of a Planar Pneumatic Manipulator. *Int. J. Robot. Res.* **2009**, *28*, 266–284. [CrossRef]
32. Gu, G.Y.; Zhu, L.M.; Su, C.Y.; Ding, H.; Fatikow, S. Proxy-based sliding-mode tracking control of piezoelectric-actuated nanopositioning stages. *IEEE/ASME Trans. Mechatron.* **2015**, *20*, 1956–1965. [CrossRef]